Dalton Transactions

Cite this: *Dalton Trans.*, 2011, **40**, 1286

www.rsc.org/dalton

PAPER

Concentration dependent tautomerism in green [Cu(HL^1)(L^2)] and brown [Cu(L^1)(HL^2)] with H_2L^1 = (*E*)-*N*′-(2-hydroxy-3-methoxybenzylidene)-benzoylhydrazone and HL^2 = pyridine-4-carboxylic (isonicotinic) acid†‡

Hassan Hosseini Monfared,*[a] Morteza Vahedpour,[a] Mahdi Mahdavi Yeganeh,[a] Massomeh Ghorbanloo,[a] Peter Mayer[b] and Christoph Janiak[c,d]

Received 26th April 2010, Accepted 9th November 2010
DOI: 10.1039/c0dt00371a

The *in situ* formed hydrazone Schiff base ligand (*E*)-*N*′-(2-hydroxy-3-methoxybenzylidene)-benzoylhydrazone (H_2L^1) reacts with copper(II) acetate in ethanol in the presence of pyridine-4-carboxylic acid (isonicotinic acid, HL^2) to green-[Cu(HL^1)(L^2)]·H_2O·C_2H_5OH (**1**) and brown-[Cu(L^1)(HL^2)] (**2**) complexes which crystallize as concomitant tautomers where either the mono-anion (HL^1)$^-$ or di-anion (L^1)$^{2-}$ of the Schiff base and simultaneously the pyridine-carboxylate (L^2)$^-$ or the acid (HL^2) (both through the pyridine nitrogen atom) function as ligands. The square-planar molecular copper(II) complexes differ in only a localized proton position either on the amide nitrogen of the hydrazone Schiff base in **1** or on the carboxyl group of the isonicotin ligand in **2**. The proportion of the tautomeric forms in the crystalline solid-state can be controlled over a wide range from **1**:**2** = 95 : 5 to ~2 : 98 by increasing the solution concentration. UV/Vis spectral studies show both tautomers to be kinetically stable (inert), that is, with no apparent tautomerization, in acetonitrile solution. The UB3LYP/6-31+G* level optimized structures of the two complexes are in close agreement with experimental findings. The solid-state structures feature 1D hydrogen-bonded chain from charge-assisted O$^{(-)}$ · · · H–N and O–H · · · $^{(-)}$N hydrogen bonding in **1** and **2**, respectively. In **1** pyridine-4-carboxylate also assumes a metal-bridging action by coordinating a weakly bound carboxylate group as a fifth ligand to a Cu axial site. Neighboring chains in **1** and **2** are connected by strong π-stacking interactions involving also the five- and six-membered, presumably metalloaromatic Cu-chelate rings.

Introduction

The rare tautomers of the naturally occurring nucleobases have been the subject of numerous studies with respect to their possible biological role in base-mispairing and mutagenesis,[1,2] and their physical properties such as relative energy, geometry, acidity, *etc.*[3] Apart from detection problems of rare tautomers present in proportions lower than 10^{-4}, a major difficulty with quantum-mechanical calculations on relative energies of tautomers represents the geometry approximation used for the respective tautomers.[4,5] Reactions of metal ions with nucleobases, hence with mixtures containing an excess of the preferred major tautomer and a tiny amount of the rare tautomer, can lead to a product containing exclusively the minor tautomer.[6–11] In the coordination chemistry of nucleobases the metal, non-coordinated counter-anion, reaction time, pH, packing factors, non-covalent interactions and solvent were found to exert an influence on tautomer selection.[12–14] Non-nucleobase examples of tautomers in metal complexes include a temperature-dependent equilibrium between $[Os(\eta^2\text{-}H_2)(CO)(quS)(PPh_3)_2]^+$ and $[Os(H)(CO)(quSH)(PPh_3)_2]^+$ (quS = quinolin-8-thiolate)[15] and an excited state intramolecular proton transfer (ESIPT) of a Schiff base to a keto tautomer to give a proficient binding capability and selectivity for fluorescent Mg^{2+} sensing (see Appendix S1 in ESI‡ for further details also on metal-nucleobase tautomers).[16]

Hydrazone derivatives inhibit DNA synthesis and cell growth.[17] Salicylaldehyde benzoylhydrazone (H_2sb) possesses mild bacteriostatic activity,[18] with its copper(II) complex being even significantly

[a]*Department of Chemistry, Faculty of Sciences, Zanjan University, 45195-313, Zanjan, I.R. Iran.. E-mail: monfared@znu.ac.ir*
[b]*Fakultät für Chemie und Pharmazie, Ludwig-Maximilians-Universität, München, Butenandtstr. 5-13, Haus D, D-81377, München, Germany*
[c]*Institut für Anorganische und Analytische Chemie, Universität Freiburg, Albertstr., 21, 79104, Freiburg, Germany*
[d]*New address: Institut für Anorganische Chemie und Strukturchemie, Universität Düsseldorf, Universitätsstr. 1, 40225, Düsseldorf, Germany. E-mail: janiak@uni-duesseldorf.de*

† Dedicated to Prof. Dr Peter Klüfers on the occasion of his 60th birthday

‡ Electronic supplementary information (ESI) available: IR spectra, enlarged UV-Vis, enlarged and additional orbital plots, crystal pictures of **1** and **2**. CCDC reference numbers 720068 and 720069. For ESI and crystallographic data in CIF or other electronic format see DOI: 10.1039/c0dt00371a

more potent, so that the metal complex was suggested as the biologically active species. Salicylaldehyde acetylhydrazone (H_2sa, Scheme 1) displays radioprotective properties,[19] and a range of acylhydrazones are cytotoxic,[20] the copper complexes again showing enhanced activity. Structural studies of copper complexes with benzoylhydrazone and analogs showed these diprotic ligands to act as tridentate, planar chelate ligands coordinating through the phenolic and amide oxygen and the imine nitrogen atom.[21] The ligand deprotonation state depends upon the conditions and metal employed.[22,23] With Cu(II) in basic media, both the phenolic and amide protons are ionized; in neutral and mild acidic solution the ligands are monoanionic, whereas strongly acidic conditions are necessary to form compounds with a neutral ligand.

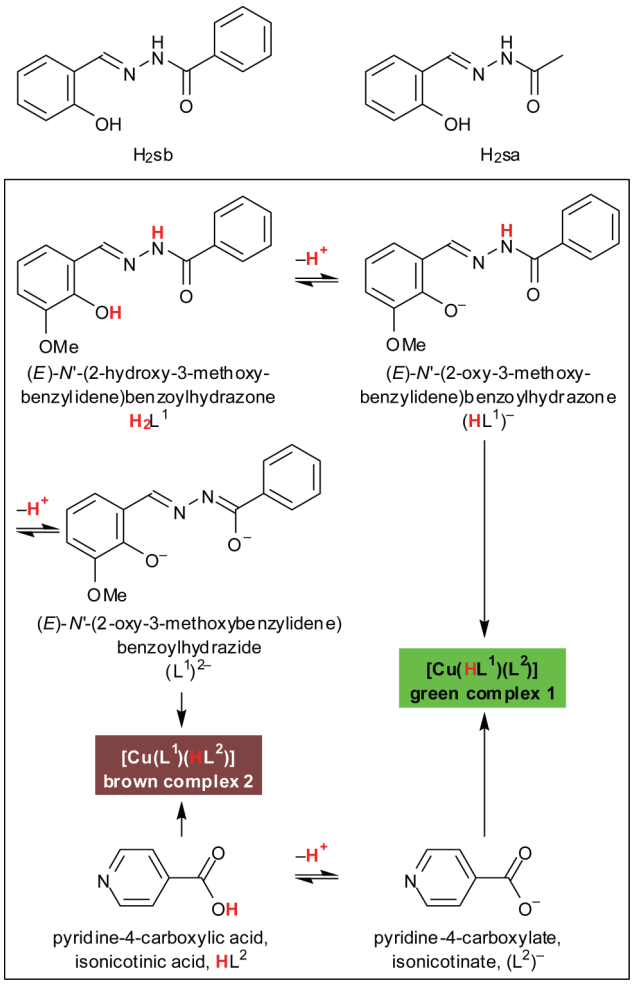

Scheme 1 Ligands and their protic equilibria relevant to the tautomeric complex formation.

Here, we report the synthesis, structures and theoretical calculations of two concomitant tautomeric copper(II) complexes with benzoylhydrazone and isonicotinic acid where the proportion of the tautomeric forms in the solid-state can be controlled over a wide range by the solution concentration.

Results and discussion

The hydrazone pro-ligand H_2L^1 was obtained by the *in situ* condensation of 2-hydroxy-3-methoxy-benzaldehyde and benzhydrazide

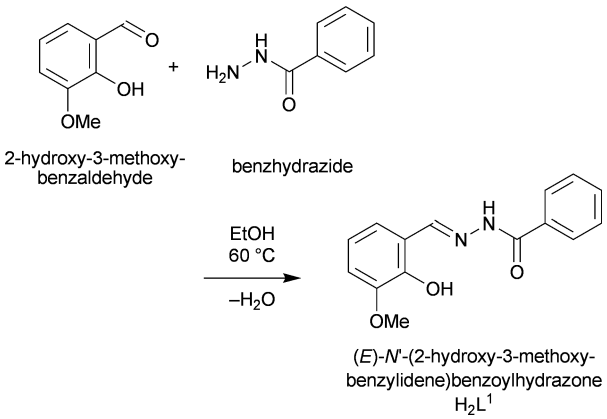

Scheme 2 *In situ* synthesis of H_2L^1.

(Scheme 2). By potentiometric titration the acidity constant pK_{a1} of the phenolic hydroxy group is about 9.00, whereas the pK_{a2} value obtained for the second amide acidity constant is 10.92 in MeOH–H_2O (0.9/0.1 v/v) at 25.0 °C.[24] The pK_a value for pyridine-4-carboxylic acid (isonicotinic acid, $HL^2 \leftrightarrows H^+ + (L^2)^-$) in H_2O at 25 °C ranges from 4.8 to 4.9 depending on the method of determination and the ionic strength of the solution (μ = 0.0 to 2.0).[25,26] While isonicotinic acid appears to be the strongest acid and should be deprotonated first, metal complexation will affect the pK_a values or protonation equilibria. Also, the solid-state composition, discussed below, is primarily influenced by the solubility and not necessarily by the solution composition.[27]

The hydrazone H_2L^1 shows IR bands assigned to ν (OH) (3563 cm^{-1}), ν (NH) (3377 and 3215 cm^{-1}), ν(C═O) (1654 cm^{-1}), and ν (C═N) + amide (1608–1576 cm^{-1}). On complexation the ν(C═O) and ν(C═N) + amide bands for the ligand are shifted, showing that coordination involves the carbonyl-O and imine-N atoms (Fig. S1 and S2 in ESI‡).

The potentially tridentate hydrazone Schiff base H_2L^1, reacts readily with Cu(II) acetate to occupy three coordination sites as an *O*,*N*,*O* donor ligand.[23] H_2L^1 in the presence of pyridine-4-carboxylic acid (HL^2) results in precipitation of green $[Cu(HL^1)(L^2)]\cdot H_2O\cdot C_2H_5OH$ (**1**) and brown $[Cu(L^1)(HL^2)]$ (**2**) where either the mono-anion $(HL^1)^-$ or di-anion $(L^1)^{2-}$ of the Schiff base functions as a ligand (Scheme 1 and 3). The ratio of **1** to **2** in the crystalline solid depends on the solution concentration from which they are crystallized. Benzhydrazide, 3-hydroxy-2-methoxy-benzaldehyde, 4-pyridinecarboxylic acid and $Cu(O_2CCH_3)\cdot H_2O$ with 0.15 : 0.13 : 0.325 : 0.15 molar ratios in 13 ml of ethanol crystallized green-**1** as the major and brown-**2** as the minor tautomer in 95 : 5 ratio. By doubling the concentration of starting reagents (doubled molar amounts in same volume) both tautomers crystallized in about equal amounts. A further doubling to 0.6 : 0.52 : 1.30 : 0.60 mmol/13 mL yielded brown-**2** as the major and a only a tiny amount of the green-**1** tautomer.

An UV-Vis spectral study of both tautomers in acetonitrile solution does not show an interconversion or equilibration. The individual spectra of **1** or **2** (*cf.* Fig. 9 and 10) do not change over a period of 2 weeks. We note that the green color of **1** is similar to the green color of $[Cu(L^1)(\mu\text{-nic})Cu(L^1)(nic)]$ or $[Cu(L^1)(nic)]$ in solution which also contains the di-anionic $(L^1)^{2-}$ ligand (nic = nicotinamide).[23]

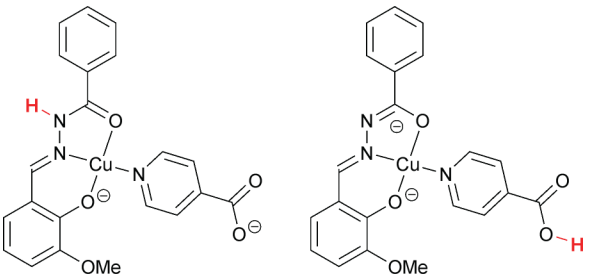

Scheme 3 Tautomeric forms of the molecular complexes in **1** and **2**.

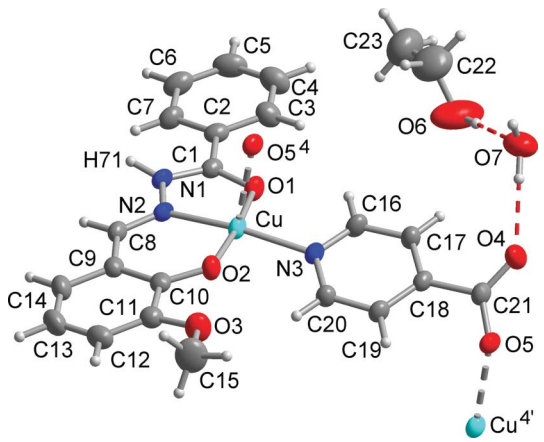

Fig. 1 Thermal ellipsoid plot (50% probability) of the repeat unit in the green compound $[Cu(HL^1)(L^2)]\cdot H_2O\cdot C_2H_5OH$ (**1**) with part of the hydrogen bonding scheme (dashed lines); bond lengths and angles in Table 1 and 2; symmetry transformations 4 = x, 0.5 – y, –0.5 + z; 4′ = x, 0.5 – y, 0.5 + z.

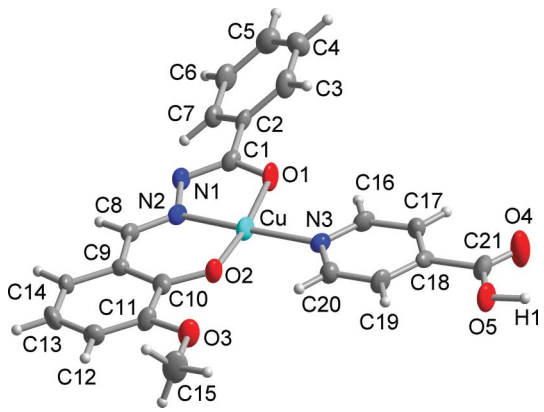

Fig. 2 Thermal ellipsoid plot (50% probability) of the brown complex $[Cu(L^1)(HL^2)]$ (**2**); bond lengths and angles in Table 1.

The molecular structures are depicted in Fig. 1 and 2, respectively (*cf.* also Scheme 3). In both compounds the Schiff base ligand forms one six-membered and one five-membered chelate ring. The dihedral angle between these two ring planes is 2.6° and 5.8° for **1** and **2**, respectively. The fourth site in the approximately square planar copper coordination sphere is occupied by the nitrogen atom from pyridine-4-carboxylate $(L^2)^-$ in **1** or its acid HL^2 in **2**. The bond lengths in **1** and **2** (Table 1) are within the expected range for copper(II) complexes with Schiff base ligands.[28] The

Table 1 Selected bond lengths (Å) and angles (°) for **1** and **2**

	green-**1**	brown-**2**
Cu–O1	1.9878(15)	1.920(3)
Cu–O2	1.8881(15)	1.871(3)
Cu–N2	1.9325(17)	1.914(3)
Cu–N3	1.9951(17)	2.006(3)
Cu–$O5^4$	2.3539(15)	—
N1–N2	1.383(3)	1.402(4)
N1–C1	1.343(3) (NH–C)	1.310(4) (–N=C)
C1–O1	1.262(3) (C=O)	1.314(4) ($C–O^{(-)}$)
O2–C10	1.312(3)	1.323(5)
N2–C8	1.295(3	1.291(5)
O1–Cu–O2	171.67(6)	171.4(1)
O1–Cu–N2	80.75(7)	81.7(1)
O1–Cu–N3	93.14(6)	92.8(1)
O2–Cu–N2	91.78(7)	94.0(1)
O2–Cu–N3	93.49(7)	92.0(1)
N2–Cu–N3	167.56(6)	173.0(2)
O1–Cu–$O5^4$	88.07(6)	—
O2–Cu–$O5^4$	96.56(6)	—
$O5^4$–Cu–N2	97.24(6)	—
$O5^4$–Cu–N3	93.34(6)	—
Cu–O1–C1	112.32(14)	111.5(3)
Cu–O2–C10	127.46(14)	126.6(2)
$Cu^{4'}$-O5–C21	130.22(13)	—

Symmetry transformations: 4 = x, 0.5 – y, –0.5 + z; 4′ = x, 0.5 – y, 0.5 + z.

Table 2 Hydrogen bonding interactions for **1** and **2**[a]

D–H···A	D–H/Å	H···A/Å	D···A/Å	D–H···A (°)
compound **1**:				
N1–H71···$O5^2$	0.89(3)	1.76(3)	2.650(2)	172(2)
OH_2···A:				
O7–H72···$O6^4$	0.73(4)	2.00(4)	2.729(4)	177(5)
O7–H73···O4	0.88(4)	1.92(5)	2.788(3)	170(4)
EtOH···A:				
O6–H86···O7	0.72(3)	1.99(3)	2.707(4)	173(4)
compound **2**:				
O5–H1···$N1^{4'}$	0.98(5)	1.66(5)	2.623(4)	168(4)

[a] D = Donor, A = Acceptor. For found and refined atoms the standard deviations are given. Symmetry transformations: 2 = 2 – x, –0.5 + y, 1.5 – z; 4 = x, 0.5 – y, –0.5 + z. 4′ = x, 0.5 – y, 0.5 + z.

N1–C1–O1 bond length variations agree with a valence structure description of –NH–C=O in **1** and $–N=C–O^{(-)} \leftrightarrow –N^{(-)}–C=O$ in **2** (calculated Mulliken charge densities for the amide N = –0.410 and O = –0.529) (Table 1).

Thus, complexes **1** and **2** show a case of tautomerism with the proton being either on the amide nitrogen of the hydrazone Schiff base ligand in **1** or on the carboxyl group of the pyridinecarboxylate ligand in **2** (Scheme 3, Fig. 1 and 2).

Adjacent molecules of **1** and **2** are connected together by charge-assisted[29] $O^{(-)}\cdots$H–N and O–H$\cdots{}^{(-)}$N hydrogen bonding, respectively, which leads to infinite hydrogen-bonded 1D chains (Fig. 3, Table 2). In **2** the charge-assistance derives from the sizable charge delocalization between the benzoyl-oxygen and the hydrazone amide nitrogen atom according to the above valence description. While a comparison of the molecular structures of **1** and **2** shows the tautomeric H atom on opposite ends of the molecules, the packing along the H-bonded chain suggests the possibility of a small H atom movement to interconvert between **1** and **2** in the solid-state (Fig. 3).

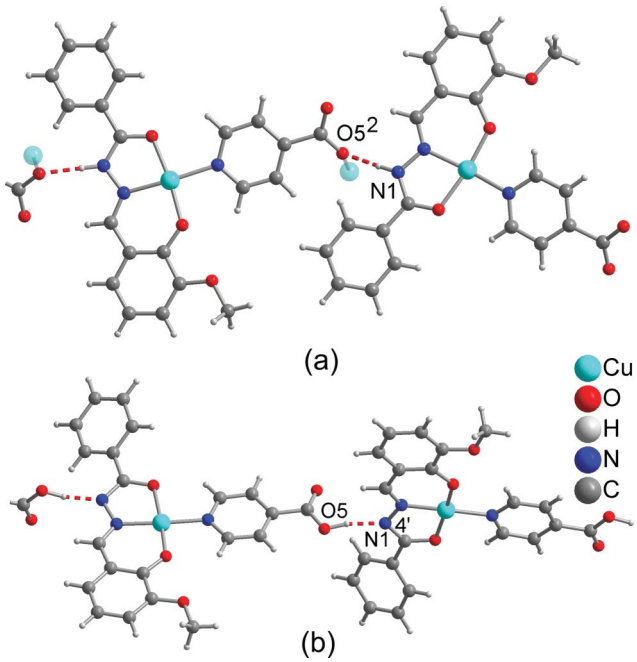

Fig. 3 Charge-assisted hydrogen-bonded molecules of (a) **1** and (b) **2** along 1D chains. The semi-transparent Cu atoms in (a) indicate the simultaneous Cu coordination of this carboxylate O atom.

In **1** the carboxylate group accepts a hydrogen bond (Fig. 3a) and also adds as a fifth, axial ligand to a nearby Cu atom which then assumes a square-pyramidal coordination sphere (Fig. 1). The bridging κ*N*:κ*O* action of the isonicotinate ligand $(L^2)^-$ between two Cu(II) atoms leads to another 1D, now {Cu(μ-L^2)} zigzag chain in **1** (Fig. 4a). The repeat units in this coordination-polymeric chain are related by glide-plane symmetry.

Pyridine-4-carboxylate [isonicotinate (L^2)] is an *N*,*O*-donor ligand,[30] and many metal coordination polymers containing this bridging ligand have been reported,[31,32] including several Cu–L^2 coordination polymers which contain a combination of isonicotinate and a bipyridyl-type ligand such as 2,2′-bipyridine, 1,10-(1,4-butanediyl)bis(imidazole), or *trans*-1,2-bis(4-pyridyl)ethylene.[33]

Neighboring {Cu(μ-L^2)}-chains in **1** interdigitate through the aforementioned N–H···O hydrogen-bonding and strong π-stacking interactions (Fig. 4b, Table 2 and Table S1 in ESI‡).

Strong π-stacking shows rather short centroid-centroid contacts (Ct···Ct < 3.8 Å) and small slip angles (β, $\gamma < 25°$) which translate into a sizable overlap of the aromatic planes. In comparison, π-stacking interactions can be viewed as medium to weak if they exhibit rather long centroid-centroid distances (Ct···Ct > 4.0 Å) together with large slip angles (β, $\gamma > 30°$).[34–36,39] π-Stacking in **1** takes place between the tilted pyridyl planes within a chain and between the interdigitated copper-benzoylhydrazone planes (Fig. 4 and 5a). The latter involves π-overlap between the benzoyl (ring 4) and copper-chelate ring planes (ring 1 and 2 in Fig. 5a). *Masui* had suggested an active electron delocalization within a metal-*N*-heterocyclic chelate ring in such a way that it could exhibit some degree of "metalloaromaticity".[23,37–39]

In complex **2** there is *no* additional axial coordination to the square-planar coordinated copper atom (Fig. 6). The dihedral angle of the coordination planes around Cu of adjacent complexes along the H-bonded chain is 86.3°. Parallel strands along *a* exhibit

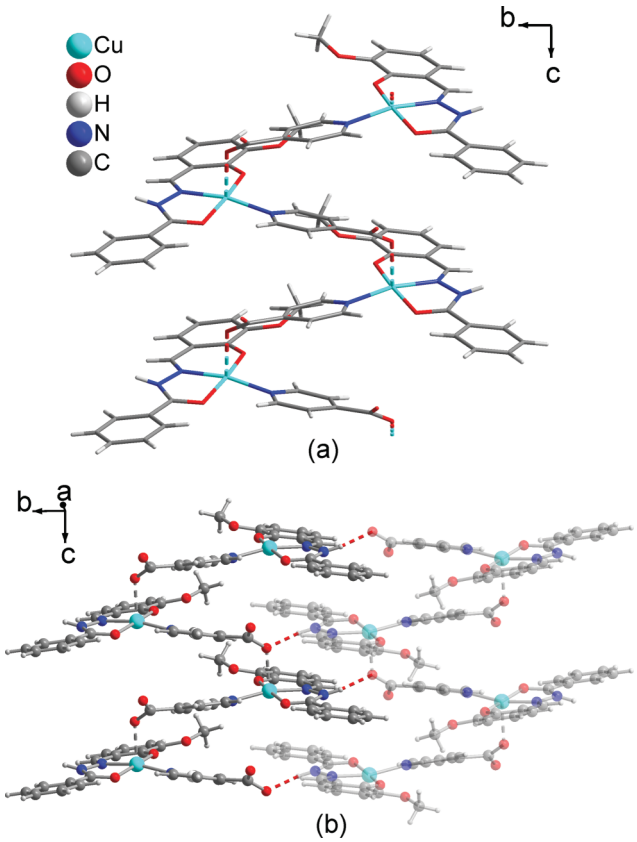

Fig. 4 (a) Section of a {Cu(μ-L^2)}-chain of **1**, following the glide plane along the *c* axis; (b) interdigitation of neighboring chains (one semi-transparent) with N–H···O hydrogen bonds as dashed red lines (*cf.* Table 2 and Fig. 3).

strong π-stacking between the five- and six-membered copper-chelate ring planes (ring 1 and 2) and the salicyl ring (Fig. 5b). Along *b* the antiparallel strands interdigitate through van der Waals interactions (Fig. 6). No significant C–H···π contacts[40] were found in the crystal packing of the strands of **1** or **2**.[45]

Molecular structure calculations

On the basis of the X-ray studies of **1** and **2**, the molecular geometries and topological properties of the copper coordination spheres were calculated with density functional theory (DFT). In complex **1**, we have used a neutral methanol molecule ($HOCH_3$) instead of the weakly bound pyridine-4-carboxylate O5 atom in the axial Cu site. This replacement resulted in a little unharmonicity in the calculated structural properties around the OCH_3 moiety. Calculations for **1** and **2** were performed in the UB3LYP (unrestricted Becke 3-parameter hybrid exchange and Lee–Yang–Parr correlation density functional) method in conjugation with the 6-31+G* level. The most relevant calculated bond lengths and their comparison with experimental values are listed in Table 3 for **1** and **2** with a maximum of 4.7 and 5.6% error. The calculated bond lengths of the complexes with the UB3LYP level of theory are within the acceptable deviation from the corresponding experimental values.

The calculations show variations in bond lengths around Cu (bond length Cu–N3 > Cu–N2, and Cu–O1> Cu–O2) that match the experimental ordering.

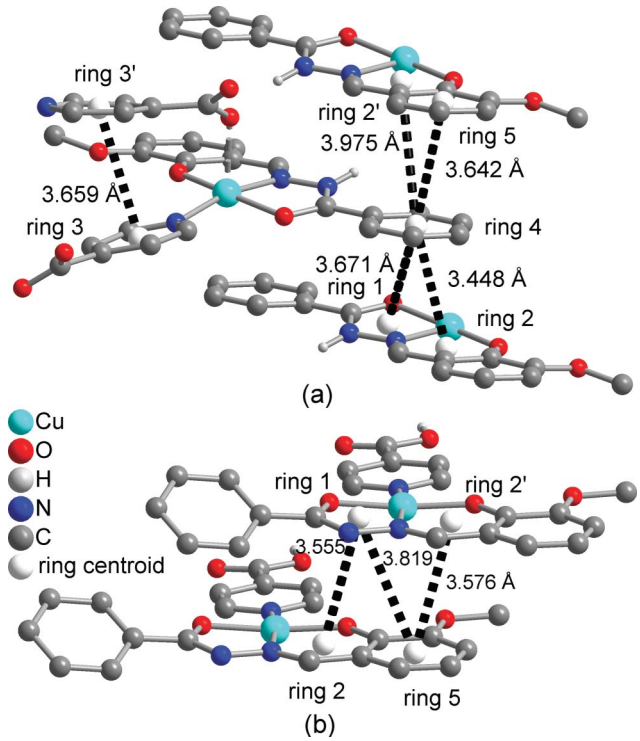

Fig. 5 Strong π-interactions in (a) **1** and (b) **2**, with the centroid-centroid contacts and ring notations given, see Table S1 in ESI‡ for further details.

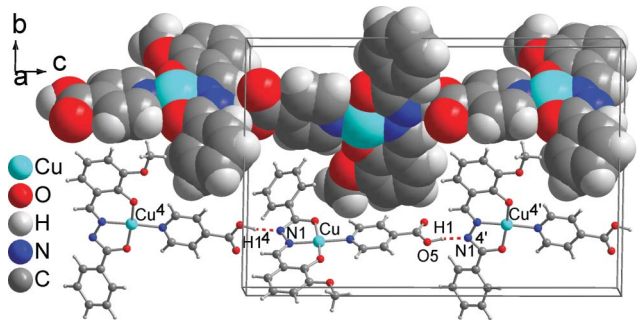

Fig. 6 Packing diagram of **2** with one hydrogen-bonded chain in ball-and-stick (bottom) and one in space-filling (top) representation. Hydrogen bonds as red dashed lines (*cf.* Table 2). Symmetry transformations 4 = x, 0.5 – y, –0.5 + z; 4′ = x, 0.5 – y, 0.5 + z.

Atom in molecule theory

Several excellent reviews have been published on the theory of atoms in molecules (AIM) developed by Bader[41] that is based on the critical points (CP) of the molecular electronic charge density, ρ(r). Four types of CP are of interest in molecules. One of them are the bond critical points, BCP, which correspond to a maximum in ρ(r) characterized by $\nabla^2\rho(r)$, and occur between two neighboring nuclei indicating the existence of a bond between them. It has been proven that AIM provides valuable information about many different chemical systems by analysis of the molecular electron density distribution. The positive value of the Laplacian ($\nabla^2\rho(r)$) according to the BCP indicates a weak interaction or an ionic bond, and the negative value of the Laplacian shows a strong covalent bond between the atoms. The bond order between two nuclei is related to the absolute value of the Laplacian and the electronic charge density value ρ(r) on bond critical points.

The values of bond critical point parameters and electron density gradient ($\nabla^2\rho(r)$), which satisfy our criteria for important bonds, are tabulated in Table 3 for complexes **1** and **2**. For both complexes positive values of the Laplacian density ($\nabla^2\rho(r) > 0$) show ionic bonds between Cu and the coordinating donor atoms. In complex **2** a bond order of Cu–N3 < Cu–O1 < Cu–N2 < Cu–O2 is seen in the electron charge density ρ(r) at the critical point of the Cu–N/O bonds which is in consistent with the inversely proportional decrease in bond lengths from Cu–N3 to Cu–O2.

For complex **1** the strength of Cu–N3, Cu–N2, Cu–O2 and Cu–O1 bonds are similar with ρ(r) = 0.1097, 0.1085, 0.1047 and 0.07459 au, respectively. Our calculation gives the electron charge density of the Cu–N3 bond as the largest value, so this bond would be the strongest of the Cu(II)-N/O bonds. The Cu–O1 in **1** is to the amide carbonyl group and experimentally longer by 0.1 Å than the Cu–O2-oxy bond. As expected, the Cu–O1 bond in **1** is the longest of all four Cu–O bonds in the two complexes. All other negative density gradients and electron charge densities in bond critical points show bonds with covalent character.

In the green complex **1** the C21–O4 and C21–O5 bond strengths correlate with the electron charge densities ρ(r) = 0.3521 and 0.3508 au, respectively, in the brown complex **2** the C21–O4 and C21–O5 bond strengths have the electron charge densities ρ(r) = 0.3995 and 0.2819 au, respectively. These results are in agreement with the experimental finding of a bond length C21–O4 (1.204 Å) in **2** that is shorter (hence stronger) than the C21–O4 bond length (1.234 Å) in **1**.

In addition, the electron charge densities for C21–O4 and C21–O5 bonds in **1** are not the same, so the resonance in this carboxylate group does not give the same bond lengths. We may conclude that the higher single bond character in the C21–O5 bond makes the O5 atom susceptible to bridge to the other Cu atom as is observed experimentally.

The ellipticity is a measure of the ratio of the rate of density decrease in the two directions perpendicular to the bond path at the bond critical point, the general shape of the bond and the degree of π-character. A value of zero indicates a symmetrical distribution of density about the bond path, such as found in standard single and triple bonds, while large values indicate a preference for density build up in a particular orientation. The values for the ellipticity for **1** and **2** are listed in Table 3.

For the green-**1** complex, the lowest ellipticity (ε) and, thus, π bonding character may be ascribed to the to the O1–C1 and O2–C10 bonds of the coordinating atoms (Table 3) whereas the highest ones belong to the N3–C20, and N3–C16 bonds, with the highest π bond contributions. In the coordination environment of Cu(II), the ellipticity in the five-membered metallacycle (Cu–N2 and Cu–O1) is greater than in the six-membered one Cu–O2 and Cu–N3, receptively. For the brown-**2** complex, the highest ellipticity (ε) and, thus, π bonding character may be ascribed to the C21–O5 and C9–C10 bonds (Table 3) whereas the lowest ones belong to the N2–C8 and O4–C21 bonds, with the lowest π bond contributions. In the coordination environment of Cu(II), the ellipticities are on the order Cu–N3 > six-membered metallacycle (Cu–N2 and Cu–O2) > five-membered metallacycle. Overall, the degree of π-character resulting from conjugation and hyperconjugation in **2** is higher than in **1**.

Table 3 Bond lengths and topological analysis of complexes **1** and **2**

green-**1** bonds	ρ(r)[a]	$\nabla^2\rho(r)$[b]	Bond lengths (calc)/Å	Bond lengths (exp)/Å	Relative error in bond lengths [%]	Ellipticity (ε)
Cu–N3	0.1097	0.4609	1.9018	1.9951	4.7	0.0079
Cu–N2	0.1085	0.5396	1.8860	1.9325	2.4	0.0139
Cu–O2	0.1047	0.6001	1.8503	1.8881	2.0	0.0342
Cu–O1	0.0746	0.3597	1.9953	1.9878	–0.37	0.0411
N3–C16	0.2980	–0.7850	1.3679	1.339	–2.1	0.0527
N3–C20	0.2968	–0.7705	1.3687	1.346	–1.7	0.0273
O1–C1	0.3427	–0.6591	1.2795	1.262	–1.4	0.0137
N2–N1	0.2868	–0.2992	1.4178	1.383	–2.5	0.1014
N2–C8	0.3265	–0.7559	1.3201	1.295	–1.9	0.0612
O2–C10	0.3427	–0.6591	1.3089	1.312	0.23	0.0137
C21–O4	0.3521	–0.6622	1.2691	1.234	–2.8	0.0272
C21–O5	0.3508	–0.6692	1.2708	1.274	0.25	0.0269
N1–C1	0.3081	–0.8297	1.3539	1.343	–0.81	0.0635
N1–H	0.2621	–0.5508	1.4630	0.893	0.54	0.0775
C1–C2	0.2830	–0.6424	1.4154	1.471	0.88	0.1379
C8–C9	0.2786	–0.5966	1.4299	1.428	–1.3	0.1522
C9–C10	0.1097	0.4609	1.9018	1.411	4.7	0.0079
brown-**2** bonds						
Cu–N3	0.07258	0.3549	2.055	2.006	–2.443	0.1129
Cu–N2	0.08475	0.4258	1.934	1.914	–1.045	0.0731
Cu–O2	0.09014	0.5905	1.894	1.871	–1.229	0.0775
Cu–O1	0.08197	0.4658	1.943	1.920	–1.198	0.0245
N3–C16	0.3151	–0.8016	1.347	1.340	–0.522	0.0486
N3–C20	0.3142	–0.7639	1.347	1.331	–1.202	0.0776
O1–C1	0.3109	–0.6529	1.308	1.314	0.457	0.1385
N2–N1	0.2981	–0.3650	1.378	1.402	1.712	0.0339
O2–C10	0.3062	–0.5440	1.311	1.323	0.907	0.1074
N2–C8	0.3597	–0.7374	1.300	1.291	–0.697	0.0133
C21–O4	0.3995	–0.4554	1.213	1.204	–0.748	0.0134
C21–O5	0.2819	–0.4594	1.354	1.282	–5.616	0.2026
N1–C1	0.3607	–1.2162	1.319	1.318	–0.076	0.0983
O5–H	0.3438	–1.7361	0.976	0.98	0.408	0.0168
C1–C2	0.2577	–0.5590	1.486	1.466	–1.364	0.0536
C8–C9	0.2657	–0.5870	1.438	1.416	–1.554	0.0796
C9–C10	0.2907	–0.6780	1.428	1.417	–0.776	0.1731

[a] Electron density (e Å^{-3}). [b] Laplacian of electron density (e Å^{-5}).

The frontier molecular orbitals of green-**1** are depicted in Fig. 7. The lowest unoccupied molecular orbital (LUMO) is an out-of-phase combination of the out-of-plane oxygen atomic p-orbitals of the carboxylate group and the LUMO+1 is primarily localized on the phenoxide/benzoyl rings and imine nitrogen atom (π*-type MOs). The highest occupied MO (HOMO) is mainly composed from phenoxide ring π-type MOs and the HOMO–1 from the in-plane carboxylate oxygen donor p-orbitals.

The frontier molecular orbitals of brown-**2** are depicted in Fig. 8. The LUMO and LUMO+1 are primarily localized on the HL^2 and L^1 rings as π*-MOs. The HOMO and HOMO–1 are mainly composed from the π-MOs of the phenoxide and hydrazido-imine moiety of L^1.

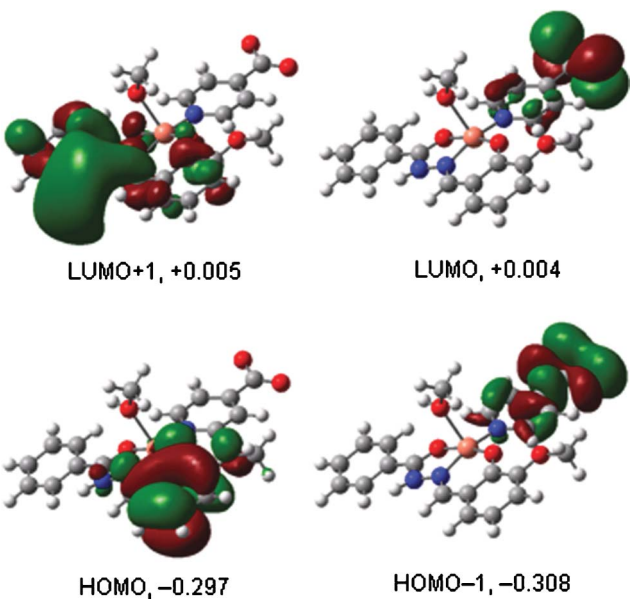

Fig. 7 Frontier molecular orbitals of green-**1** with the energy eigenvalues in eV; additional orbitals are given in Fig. S4 in the ESI‡.

Conclusions

The ratio of two crystallized concomitant tautomeric complexes green-$[Cu(HL^1)(L^2)]\cdot H_2O\cdot C_2H_5OH$ (**1**) and brown-$[Cu(L^1)(HL^2)]$ (**2**) can be influenced by the concentration of the reactants. A lower concentration increases the proportion of the solvent-containing tautomer **1**. In an aprotic solvent both forms are inert, with no apparent tautomerization.

DFT-calculated bond lengths are in close agreement with experimental findings and the positive value of the Laplacian ($\nabla^2\rho(r)$) shows the Cu(II) bonds in complexes **1** and **2** to be ionic. The formation of **1** and **2** which crystallize as concomitant tautomers must be rationalized in terms of their similar total

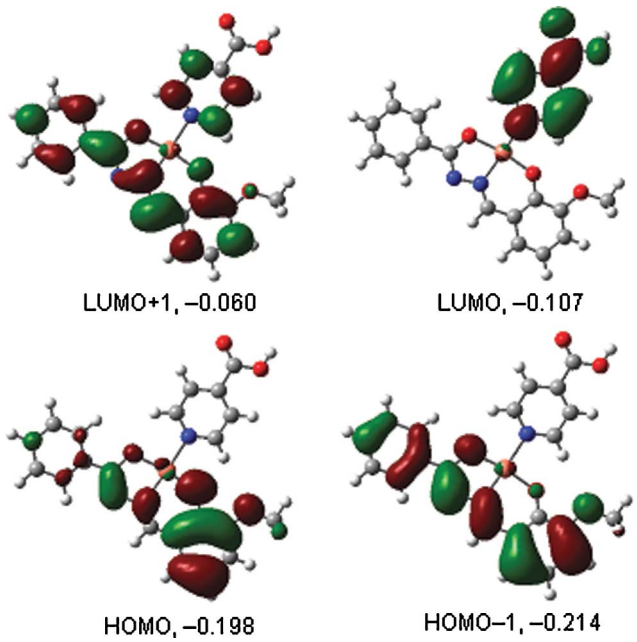

Fig. 8 Frontier molecular orbitals of brown-**2** with the energy eigenvalues in eV; additional orbitals are shown in Fig. S5 in the ESI‡.

energies which include intramolecular as well as supramolecular (H-bonding, π-stacking) contributions together with a sufficient energy barrier for interconversion (kinetic stability).

Experimental

Benzhydrazide, 2-hydroxy-3-methoxybenzaldehyde, copper(II) acetate monohydrate and solvents with high purity were purchased from Merck and Fluka and used as received. IR spectra were recorded in KBr disks with a Matson 1000 FT-IR spectrophotometer in the range of 4000–450 cm^{-1}. UV-VIS spectra of acetonitrile solutions were recorded on a Shimadzu 160 spectrometer. Microanalytical (CHN) data were obtained with a Carlo ERBA Model EA-1108 analyzer. Atomic absorption spectrometry was measured with a Varian 220 FS spectrophotometer.

[(*E*)-*N*′-((2-oxy-3-methoxybenzylidene)benzoylhydrazone-κ^3*O*,*N*,*O*′)(4-pyridinecarboxylato-κ*N*) copper(II)] monohydrate monoethanol, [Cu(HL^1)(L^2)]·H_2O·C_2H_5OH (green-1) and [(*E*)-*N*′-((2-oxy-3-methoxybenzylidene)benzoylhydrazido-κ^3*O*,*N*,*O*′)(4-pyridinecarboxylic acid-κ*N*)] copper(II)], [Cu(L^1)(HL^2)] (brown-2)

Experiment No. 1. Benzhydrazide (0.02 g, 0.15 mmol), 2-hydroxy-3-methoxybenzaldehyde (0.02 g, 0.13 mmol), 4-pyridinecarboxylic acid (0.04 g, 0.325 mmol) and copper(II) acetate monohydrate (0.03 g, 0.15 mmol) were placed in the main arm of the branched tube ('branched tube' method). Ethanol (96%, 13 mL) was carefully added to fill the arms, the tube was sealed and the reagents containing arm immersed in an oil bath at 60 °C while the other arm was kept at ambient temperature. After two weeks, a mixture of green and brown crystals was deposited in the cooler arm, which was filtered off, washed with ethanol and air dried (combined yield 0.06 g, 50% based on Cu). The pH in the beginning was 4.05, at the end of the reaction 4.07. The green (**1**) and brown (**2**) crystals were manually separated under a microscope to an about 95 : 5 ratio (Fig. S6 in ESI‡).

Experiment No. 2. Benzhydrazide (0.04 g, 0.30 mmol), 2-hydroxy-3-methoxybenzaldehyde (0.04 g, 0.26 mmol), 4-pyridinecarboxylic acid (0.08 g, 0.65 mmol) and copper(II) acetate monohydrate (0.06 g, 0.30 mmol) were placed in the main arm of the branched tube. Ethanol (96%, 13 mL) was carefully added to fill the arms, the tube was sealed and the reagents containing arm immersed in an oil bath at 60 °C while the other arm was kept at ambient temperature. After two weeks, a mixture of green and brown crystals was deposited in the cooler arm, which was filtered off, washed with ethanol and air dried (yield 55% based on Cu). The pH in the beginning was 4.05, at the end of the reaction 4.20. The green (**1**) and brown (**2**) crystals were manually separated under a microscope to an about 50 : 50 ratio (Fig. S7 in ESI‡).

Experiment No. 3. Benzhydrazide (0.08 g, 0.60 mmol), 2-hydroxy-3-methoxybenzaldehyde (0.08 g, 0.52 mmol), 4-pyridinecarboxylic acid (0.16 g, 1.30 mmol) and copper(II) acetate monohydrate (0.12 g, 0.60 mmol) were placed in the main arm of the branched tube. Ethanol (96%, 13 mL) was carefully added to fill the arms, the tube was sealed and the reagents containing arm immersed in an oil bath at 60 °C while the other arm was kept at ambient temperature. After two weeks, a mixture of green and brown crystals was deposited in the cooler arm, which was filtered off, washed with ethanol and air dried (yield 70% based on Cu). The pH in the beginning was 4.05, at the end of the reaction 4.17. The green (**1**) and brown (**2**) crystals were manually separated under a microscope to an about 2 : 98 ratio (Fig. S8 in ESI‡).

Analytical data. Mp. of green-**1** 242–243 °C (dec.), brown-**2** 277–278 °C. Calc. for green-$C_{23}H_{25}CuN_3O_7$ (**1**): C 53.23, H 4.86, Cu 12.24, N 8.10; found: C 53.23, H, 4.40, Cu 12.50, N 8.20%. Calc. for brown-$C_{21}H_{17}CuN_3O_5$ (**2**): C 55.44, H 3.77, Cu 13.97, N, 9.24; found C 55.30, H 3.76, Cu 14.00, N 9.30%. IR for green-**1** (KBr, cm^{-1}): 3415 (s, br), 2923 (m), 1615 (vs), 1538 (s), 1438 (m), 1354 (s), 1331 (m), 1246 (m), 1215 (vs), 1092 (s), 984 (w), 869 (w), 746 (m), 700 (s), 454 (w) (Fig. S1 in ESI‡). IR for brown-**2** (KBr, cm^{-1}): 3854 (s), 3738 (vs), 3669 (m), 3646 (m), 3623 (m), 2923 (m), 2854 (w), 1654 (w), 1562 (w), 1462 (w), 1400 (w), 1100 (vs), 685 (w), 446 S, br) (Fig. S2 in ESI‡). UV/Vis for **1** (in CH_3CN, $c = 4.24 \times 10^{-5}$ mol L^{-1}, green solution, λ_{max} [nm] with ε [l mol^{-1} cm^{-1}]): 238 (22100), 329 (17430), 372 (8560), 393 (8610), 668 (165) (Fig. 9). The spectrum does not change over a period of 2 weeks. UV/Vis for **2** (in CH_3CN, $c = 4.84 \times 10^{-5}$ mol L^{-1}, very light brown solution, λ_{max} [nm] with ε [l mol^{-1} cm^{-1}]): 212 (17400), 274 (5600), 342 (190), 473 (190) (Fig. 10). The spectrum does not change over a period of 2 weeks.

X-ray structure determination

A suitable single crystal was carefully selected under a polarizing microscope. *Data Collection*: Nonius Kappa CCD for **1**, Oxford XCalibur diffractometer for **2**, both at a temperature of 200(2) K, Mo-Kα radiation (λ = 0.71073 Å), obtained from graded multilayer X-ray optics. The structure was solved by Direct Methods with SIR97,[42] and refined with full-matrix least-squares techniques on F^2 with SHELXL-97.[43] The crystal data and refinement parameters are presented in Table 4. The C–H hydrogen

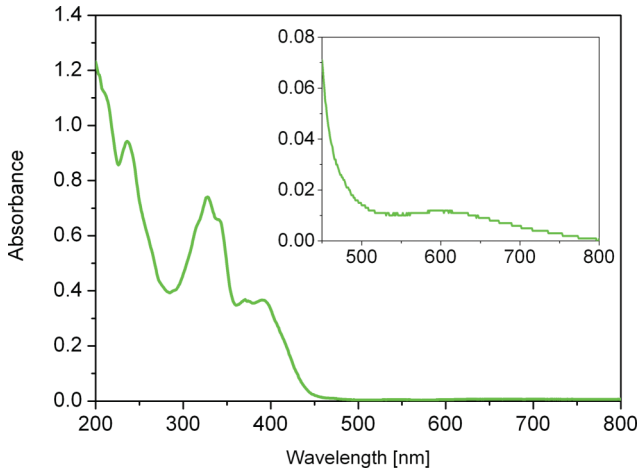

Fig. 9 UV-Vis spectrum of green-**1** in CH_3CN.

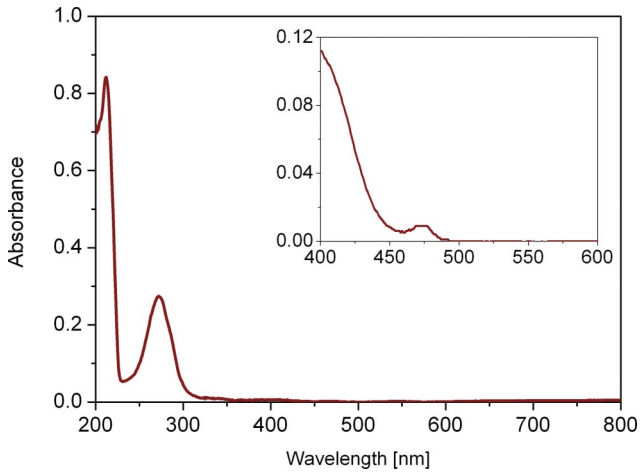

Fig. 10 UV-Vis spectrum of brown-**2** in CH_3CN.

atoms were calculated in idealized geometry riding on their parent atoms. The protic O–H and N–H atoms were found and refined. The structure plots were prepared with DIAMOND.[44] Details of the supramolecular π-interactions were calculated with the program PLATON.[45] The structural data has been deposited with the Cambridge Crystallographic Data Center (CCDC numbers 720068 for green-**1** and 720069 for brown-**2**).‡ These data can be obtained free of charge *via* www.ccdc.cam.ac.uk/datarequest/cif.

Computational methods

Geometries of complexes **1** and **2** were fully optimized with the density functional theory (DFT) method at the UB3LYP level of theory with the 6-31+G* basis set using the G03 program.[46] At the first step, we have employed semiempirical methods to optimize the complexes. The obtained results improved using the UB3LYP calculation method. At the level of this method it is possible to generate a wave function in a form suitable to execute the topological analysis atom in the molecule[47] by means of the AIM2000 series programs.[48]

Table 4 Crystal data and refinement details for **1** and **2**

Complex color	**1** green	**2** brown
net formula	$C_{23}H_{25}CuN_3O_7$	$C_{21}H_{17}CuN_3O_5$
M_r/g mol^{-1}	519.007	454.923
Crystal size/mm	0.22 × 0.14 × 0.04	0.15 × 0.07 × 0.04
Crystal system	Monoclinic	Monoclinic
Space group	$P2_1/c$	$P2_1/c$
a/Å	13.6380(3)	4.7333(3)
b/Å	23.6172(5)	16.0520(10)
c/Å	7.24590(10)	24.2371(10)
β (°)	96.1919(12)	94.195(5)
V/Å^3	2320.23(8)	1836.58(18)
Z	4	4
D_c/g cm^{-3}	1.48579(5)	1.64529(16)
μ/mm^{-1}	0.991	1.231
absorpt. correction	none	numerical
transmiss. factor range		0.7551–0.9302
refls. measured	17032	7223
R_{int}	0.0420	0.0525
mean σ(I)/I	0.0346	0.1180
θ range	3.18–26.37	3.90–24.00
observed refls.	3757	1573
x, y (weight. scheme)	0.0450, 1.2333	0.0301, 0
hydrogen refinement	mixed	mixed
refls in refinement	4735	2784
Parameters	325	276
restraints	0	0
$R(F_{obs})$	0.0351	0.0404
$R_w(F^2)$	0.0935	0.0773
Goodness-of-fit, S	1.049	0.871
shift/error$_{max}$	0.001	0.001
max electr. dens./e Å^{-3}	0.398	0.694
min electr. dens./e Å^{-3}	–0.505	–0.348

Acknowledgements

We thank the Zanjan University, the Ludwig-Maximilians-Universität and the Universität Freiburg for financial support of this study as well as the DFG for grant Ja466/14-1.

Notes and references

1 P. O. Löwdin, *Adv. Quantum Chem.*, 1965, **2**, 213; B. Pullman and A. Pullman, *Adv. Heterocycl. Chem.*, 1971, **13**, 77; M. D. Topal and J. R. Fresco, *Nature*, 1976, **263**, 285.
2 Y. Wu, R. Sa, Q. Li, Y. Wei and K. Wu, *Chem. Phys. Lett.*, 2009, **467**, 387–392.
3 J. S. Kwiatkowski and B. Pullman, *Adv. Heterocycl. Chem.*, 1975, **18**, 199.
4 R. Czerminski, B. Lesyng and A. Pohorille, *Int. J. Quantum Chem.*, 1979, **16**, 605.
5 B. Lippert, H. Schöllhorn and U. Thewalt, *J. Am. Chem. Soc.*, 1986, **108**, 6616–6621.
6 B. Lippert, *Inorg. Chim. Acta*, 1981, **55**, 5–14.
7 J.-P. Charland, M. T. P. Viet, M. St-Jacaques and A. L. Beauchamp, *J. Am. Chem. Soc.*, 1985, **107**, 8202; M. J. Clarke, *J. Am. Chem. Soc.*, 1978, **100**, 5068; L. Y. Kuo, M. G. Kanatzidis, M. Sabat, A. L. Tipton and T. J. Marks, *J. Am. Chem. Soc.*, 1991, **113**, 9027; E. F. Day, C. A. Crawford, K. Foltin, K. R. Dunbar and G. Christou, *J. Am. Chem. Soc.*, 1994, **116**, 9339; K. V. Catalan, D. J. Mindiola, D. L. Ward and K. R. Dunbar, *Inorg. Chem.*, 1997, **36**, 2458; W. Brüning, I. Ascaso, E. Freisinger, M. Sabat and B. Lippert, *Inorg. Chim. Acta*, 2002, **339**, 400–410.
8 F. Zamora, M. Kunsman, M. Sabat and B. Lippert, *Inorg. Chem.*, 1997, **36**, 1583–1587.
9 J. P. Garćıa-Terán, O. Castillo, A. Luque, U. García-Couceiro, G. Beobide and P. Román, *Dalton Trans.*, 2006, 902–911.
10 F. Pichierri, D. Holthenrich, E. Zangrando, B. Lippert and L. Randaccio, *JBIC, J. Biol. Inorg. Chem.*, 1996, **1**, 439–445.

11 Ru(III) with rare imine tautomer of 9-methyladenine: A. H. Velders, B. Geest, H. Kooijman, A. L. Spek, J. G. Haasnoot and J. Reedijk, *Eur. J. Inorg. Chem.*, 2001, 369–372.
12 (*a*) I. Mutikainen and P. Lumme, *Acta Crystallogr., Sect. B: Struct. Crystallogr. Cryst. Chem.*, 1980, **36**, 2237–2240; (*b*) R. Pfab, P. Jandik and B. Lippert, *Inorg. Chim. Acta*, 1982, **66**, 193–204; (*c*) I. Escorihuela, L. R. Falvello, M. Tomás and E. P. Urriolabeitia, *Cryst. Growth Des.*, 2004, **4**, 655–657.
13 T. Wijst, C. F. Guerra, M. Swart, F. M. Bickelhaupt and B. Lippert, *Chem.–Eur. J.*, 2009, **15**, 209–218.
14 T. F. Mastropietro, D. Armentano, N. Marino and G. D. Munno, *Polyhedron*, 2007, **26**, 4945–4954.
15 M. Schlaf and R. H. Morris, *J. Chem. Soc., Chem. Commun.*, 1995, 625.
16 N. Singh, N. Kaur, R. C. Mulrooney and J. F. Callan, *Tetrahedron Lett.*, 2008, **49**, 6690–6692.
17 L. Pickart, W. H. Goodwin, W. Burgua, T. B. Murphy and D. K. Johnson, *Biochem. Pharmacol.*, 1983, **32**, 3868–3871.
18 H. A. Offe, W. Siefken and G. Domagk, *Z. Naturforsch. B*, 1952, **7**, 462–468.
19 O. V. Arapov, O. F. Alferva, E. I. Levocheskaya and I. Krasil'nikov, *Radiobiologiya*, 1987, **27**, 843–846.
20 J. D. Ranford, J. J. Vittal and Y. M. Wang, *Inorg. Chem.*, 1998, **37**, 1226–1231.
21 A. A. Aruffo, T. B. Murphy, D. K. Johnson, N. J. Rose and V. Schomaker, *Acta Crystallogr., Sect. C: Cryst. Struct. Commun.*, 1984, **40**, 1164–1169; E. W. Ainscough, A. M. Brodie, A. Dobbs, J. D. Ranford and J. M. Waters, *Inorg. Chim. Acta*, 1995, **236**, 83–88; S. C. Chan, L. L. Koh, P.-H. Leung, J. D. Ranford and K. Y. Sim, *Inorg. Chim. Acta*, 1995, **236**, 101–108.
22 E. W. Ainscough, A. M. Brodie, A. Dobbs, J. D. Ranford and J. M. Waters, *Inorg. Chim. Acta*, 1998, **267**, 27–38.
23 H. Hosseini Monfared, Z. Kalantari, M.-A. Kamyabi and C. Janiak, *Z. Anorg. Allg. Chem.*, 2007, **633**, 1945–1948.
24 M. Ali Kamyabi, S. Shahabi and H. Hosseini-Monfared, *J. Chem. Eng. Data*, 2008, **53**, 2341–2345.
25 A. E. Martell, R. M. Smith and R. J. Motekaitis, *NIST Critically Selected Stability Constants of Metal Complexes*, Version 6.
26 A. G. Asuero, M. J. Navas, M. A. Herrador and A. F. Recamales, *Int. J. Pharm.*, 1986, **34**, 81–92.
27 E. Craven, K. Abu-Shandi and C. Janiak, *Z. Anorg. Allg. Chem.*, 2003, **629**, 195–201.
28 A. D. Garnovskii, A. L. Nivorozhkin and V. I. Minkin, *Coord. Chem. Rev.*, 1993, **126**, 1; S. Mandal, G. Das, R. Singh and K. Bhuradwaj, *Coord. Chem. Rev.*, 1997, **160**, 191.
29 B. M. Drašković, G. A. Bogdanović, M. A. Neelakantan, A.-C. Chamayou, S. Thalamuthu, Y. S. Avadhut, J. Schmedt auf der Günne, S. Banerjee and C. Janiak, *Cryst. Growth Des.*, 2010, **10**, 1665–1676; A.-C. Chamayou and C. Janiak, *Inorg. Chim. Acta*, 2010, **363**, 2193–2200; F. Zhuge, B. Wu, J. Liang, J. Yang, Y. Liu, C. Jia, C. Janiak, N. Tang and X.-J. Yang, *Inorg. Chem.*, 2009, **48**, 10249–10256; E. Redel, C. Röhr and C. Janiak, *Chem. Commun.*, 2009, 2103–2105; E. Redel, M. Fiederle and C. Janiak, *Z. Anorg. Allg. Chem.*, 2009, **635**, 1139–1147; B. Wu, J. Liang, J. Yang, C. Jia, X.-J. Yang, H. Zhang, N. Tang and C. Janiak, *Chem. Commun.*, 2008, 1762–1764; B. Wu, X. Huang, Y. Xia, X.-J. Yang and C. Janiak, *CrystEngComm*, 2007, **9**, 676–685; T. Dorn, A.-C. Chamayou and C. Janiak, *New J. Chem.*, 2006, **30**, 156–167; M. D. Ward, *Chem. Commun.*, 2005, 5838–5842; T. Dorn, C. Janiak and K. Abu-Shandi, *CrystEngComm*, 2005, **7**, 633–641.
30 C. B. Aakeröy and A. M. Beatty, in: J. A. McCleverty, T. J. Meyer (ed.), *Comprehensive Coordination Chemistry II*, vol. 1, Pergamon Press, New York, 2004, pp. 679–688.
31 C. Janiak, *Dalton Trans.*, 2003, 2781–2804.
32 L. Ma, O. W. Evans, B. M. Foxman and W. Lin, *Inorg. Chem.*, 1999, **38**, 5837; J. Y. Lu and A. M. Babb, *Chem. Commun.*, 2001, 821; M. E. Chapman, P. Ayappan, B. M. Foxman, G. T. Yee and W. Lin, *Cryst. Growth Des.*, 2001, **1**, 159; C. Z.-J. Lin, S. S.-Y. Chui, S. M.-F. Lo, F. L.-Y. Shek, M. Yu, K. Suwinka, J. Lipkowski and I. D. Williams, *Chem. Commun.*, 2002, 1642; Y. Kang, Y.-G. Yao, Y.-Y. Qin, J. Zhang, Y.-B. Chen, Z.-J. Li, Y.-H. Wen, J.-K. Cheng and R.-F. Hu, *Chem. Commun.*, 2004, 1046; X. Bai, Y. Li, E. Wang and L. Xu, *Inorg. Chim. Acta*, 2005, **358**, 2571; T.-H. Ma, J.-H. Yu, L. Ye, J.-Q. Xu, T.-G. Wang and C.-H. Lu, *J. Mol. Struct.*, 2003, **654**, 47; J.-H. Liao, C.-Y. Lai, C.-D. Ho and C.-T. Su, *Inorg. Chem. Commun.*, 2004, **7**, 402; F. T. Xie, H.-Y. Bie, L.-M. Duan, G.-H. Li, X. Zhang and J. Q. Xu, *J. Solid State Chem.*, 2005, **178**, 2858; M.-B. Zhang, J. Zhang, S.-T. Zheng and G.-Y. Yang, *Angew. Chem. Int. Ed.*, 2005, **44**, 1358.
33 A.-L. Xie and D.-J. Xu, *J. Coord. Chem.*, 2005, **58**, 225; J.-F. Ma, J. Yang, G.-L. Zheng, L. Li, Y.-M. Zhang, F.-F. Li and J.-F. Liu, *Polyhedron*, 2004, **23**, 553; J. Y. Lu and A. M. Babb, *Inorg. Chem.*, 2001, **40**, 3261.
34 C. Janiak, *J. Chem. Soc., Dalton Trans.*, 2000, 3885–3896.
35 H. A. Habib, A Hoffmann, H. A. Höppe, G. Steinfeld and C. Janiak, *Inorg. Chem.*, 2009, **48**, 2166–2180; B. Wu, X. Huang, Y. Xia, X.-J. Yang and C. Janiak, *CrystEngComm*, 2007, **9**, 676–685; B. Wisser and C. Janiak, *Acta Crystallogr., Sect. E: Struct. Rep. Online*, 2007, **63**, o2871–2872; T. Dorn, C. Janiak and K. Abu-Shandi, *CrystEngComm*, 2005, **7**, 633–641.
36 X.-J. Yang, F. Drepper, B. Wu, W.-H. Sun, W. Haehnel and C. Janiak, *Dalton Trans.*, 2005, 256–267 and supplementary material therein.
37 H. Masui, *Coord. Chem. Rev.*, 2001, **219–221**, 957.
38 A. Castiñeiras, A. G. Sicilia-Zafra, J. M. Gonzáles-Pérez, D. Choquesillo-Lazarte and J. Niclós-Gutiérrez, *Inorg. Chem.*, 2002, **41**, 6956; E. Craven, C. Zhang, C. Janiak, G. Rheinald and H. Lang, *Z. Anorg. Allg. Chem.*, 2003, **629**, 2282–2290.
39 C. Janiak, A.-C. Chamayou, A. K. M. R. Uddin, M. Uddin, K. S. Hagen and M. Enamullah, *Dalton Trans.*, 2009, 3698.
40 M. Nishio, Y. Umezawa, K. Honda, S. Tsuboyama and H. Suezawa, *CrystEngComm*, 2009, **11**, 1757; M. Nishio, *CrystEngComm*, 2004, **6**, 130; M. Nishio, M. Hirota and Y. Umezawa, *The CH/p interaction (Evidence, Nature and consequences)*, Wiley-VCH, 1998; Y. Umezawa, S. Tsuboyama, K. Honda, J. Uzawa and M. Nishio, *Bull. Chem. Soc. Jpn.*, 1998, **71**, 1207; C. Janiak, S. Temizdemir, S. Dechert, W. Deck, F. Girgsdies, J. Heinze, M. J. Kolm, T. G. Scharmann and O. M. Zipffel, *Eur. J. Inorg. Chem.*, 2000, 1229–1241.
41 P. L. A. Popelier, *Atoms in Molecules: An Introduction*, Pearson Education, Harlow, 2000.
42 A. Altomare, M. C. Burla, M. Camalli, G. L. Cascarano, C. Giacovazzo, A. Guagliardi, A. G. G. Moliterni, G. Polidori and R. Spagna, SIR97: a new tool for crystal structure determination and refinement, *J. Appl. Crystallogr.*, 1999, **32**, 115.
43 G. M. Sheldrick, *Acta Crystallogr., Sect. A: Found. Crystallogr.*, 2008, **64**, 112–122.
44 K. Brandenburg, Diamond (Version 3.2d), *Crystal and Molecular Structure Visualization, Crystal Impact* – K. Brandenburg & H. Putz Gbr, Bonn (Germany), 2009.
45 (*a*) A. L. Spek, *J. Appl. Crystallogr.*, 2003, **36**, 7–13; (*b*) PLATON – A Multipurpose Crystallographic Tool, Utrecht University, Utrecht, The Netherlands, A. L. Spek (2008); (*c*) Windows implementation: L. J. Farrugia, University of Glasgow, Scotland, Version 40608 (2008).
46 Gaussian 03, Revision B.03, M. J. Frisch, G. W. Trucks, H. B. Schlegel, G. E. Scuseria, M. A. Robb, J. R. Cheeseman, J. A. Montgomery, Jr., T. Vreven, K. N. Kudin, J. C. Burant, J. M. Millam, S. S. Iyengar, J. Tomasi, V. Barone, B. Mennucci, M. Cossi, G. Scalmani, N. Rega, G. A. Petersson, H. Nakatsuji, M. Hada, M. Ehara, K. Toyota, R. Fukuda, J. Hasegawa, M. Ishida, T. Nakajima, Y. Honda, O. Kitao, H. Nakai, M. Klene, X. Li, J. E. Knox, H. P. Hratchian, J. B. Cross, C. Adamo, J. Jaramillo, R. Gomperts, R. E. Stratmann, O. Yazyev, A. J. Austin, R. Cammi, C. Pomelli, J. W. Ochterski, P. Y. Ayala, K. Morokuma, G. A. Voth, P. Salvador, J. J. Dannenberg, V. G. Zakrzewski, S. Dapprich, A. D. Daniels, M. C. Strain, O. Farkas, D. K. Malick, A. D. Rabuck, K. Raghavachari, J. B. Foresman, J. V. Ortiz, Q. Cui, A. G. Baboul, S. Clifford, J. Cioslowski, B. B. Stefanov, G. Liu, A. Liashenko, P. Piskorz, I. Komaromi, R. L. Martin, D. J. Fox, T. Keith, M. A. Al-Laham, C. Y. Peng, A. Nanayakkara, M. Challacombe, P. M. W. Gill, B. Johnson, W. Chen, M. W. Wong, C. Gonzalez and J. A. Pople, Gaussian, Inc., Pittsburgh PA, 2003.
47 R. F. W. Bader, *Atoms* in *Molecules: A Quantum Theory*, Oxford University Press, Oxford, 1990.
48 F. Biegler-Konig and J. Schoenbohm, AIM2000, 2.0 ed., Büro für Innovative Software, Bielefeld, Germany, 2002.

